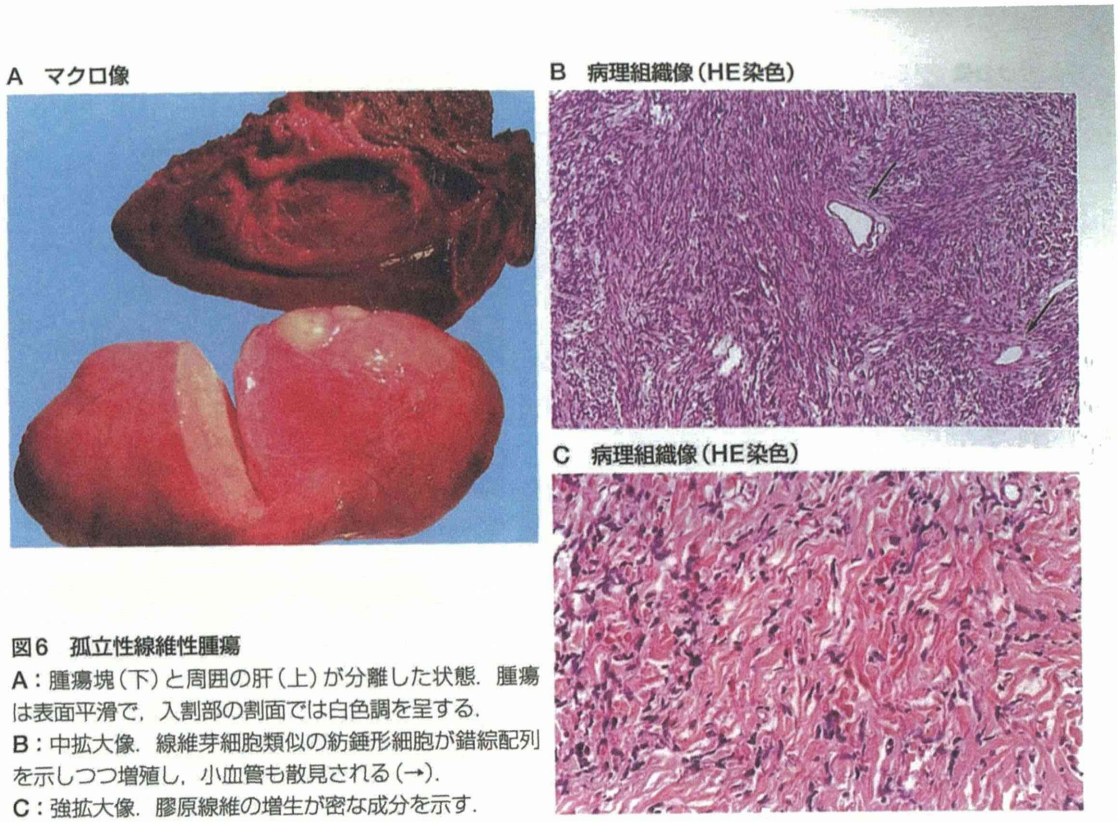

図6　孤立性線維性腫瘍
A：腫瘍塊（下）と周囲の肝（上）が分離した状態．腫瘍は表面平滑で，入割部の割面では白色調を呈する．
B：中拡大像．線維芽細胞類似の紡錘形細胞が錯綜配列を示しつつ増殖し，小血管も散見される（→）．
C：強拡大像．膠原線維の増生が密な成分を示す．

真の腫瘍か否かは結論が出ておらず，また胆管細胞腺腫と胆管周囲付属腺との表現型の類似性より，peribiliary gland hamartomaとも呼称されている[15]．

6 孤立性線維性腫瘍 (solitary fibrous tumor)

孤立性線維性腫瘍は単発性のきわめて稀な肝腫瘍で，胸膜，縦隔などに発生する本腫瘍と同様な組織像を示す．現在までの文献的報告は43症例[16]で，成人例が多く（16～84歳），やや女性に多い（男16例，女27例）．肉眼上，境界明瞭な淡黄褐色～白色のやや硬い腫瘍で，子宮筋腫類似の渦を巻いたような外観を呈し，変性や壊死，出血を混じる症例もある（図6-A）．

組織学的に，異型に乏しい線維芽細胞類似の紡錘形～卵円形細胞の増殖からなり，膠原線維や小血管が介在する（図6-B, C）．種々の細胞密度からなる部位や粘液腫様の成分も混ずる症例が多い．免疫組織化学的染色にて，腫瘍細胞はCD34, vimentin, bcl-2が陽性，CD99も陽性を示す症例がある．通常良性であるが稀に悪性転化もあり，悪性症例では壊死，細胞異型，核分裂細胞の増加を示し，CD34の染色性低下，変異型p53の発現がみられる[17]．

7 肝副腎遺残腫瘍 (adrenal rest tumor)

肝副腎遺残腫瘍は，個体発生の過程で肝に遺残した副腎組織が腫瘍化した遺残腫瘍である．副腎遺残自体は新生児の約50%に認められ，生後1年以内に退縮してほぼ消失し，成人期を通して存在するのは1%程度である．肝副腎遺残腫瘍は非機能性腫瘍であることが多く，ほとんどの症例は右葉後上区域（S_7）に存在する．

腫瘍の割面は境界明瞭で，脂質を反映して黄色調の強い腫瘤を呈する（図7-A）．組織像は通常の副腎皮質組織と同様，淡明で弱好酸性の胞体を有する大型多角形細胞が，薄い線維性隔壁を伴って胞巣状あるいは索状に増生し，血管も散見される

bcl-2：B-cell lymphoma/leukemia-2　　CD-34, 99：cluster of differentiation-34, 99

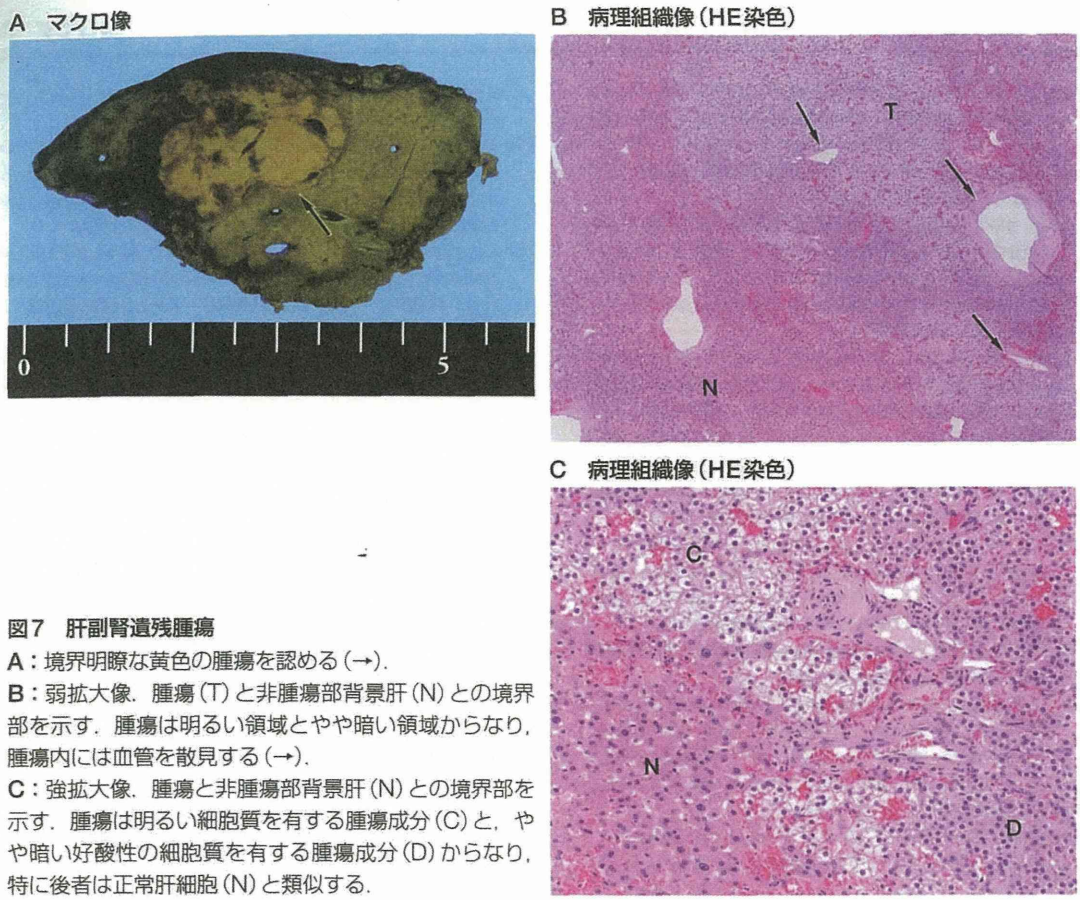

図7　肝副腎遺残腫瘍

A：境界明瞭な黄色の腫瘍を認める（→）．

B：弱拡大像．腫瘍（T）と非腫瘍部背景肝（N）との境界部を示す．腫瘍は明るい領域とやや暗い領域からなり，腫瘍内には血管を散見する（→）．

C：強拡大像．腫瘍と非腫瘍部背景肝（N）との境界部を示す．腫瘍は明るい細胞質を有する腫瘍成分（C）と，やや暗い好酸性の細胞質を有する腫瘍成分（D）からなり，特に後者は正常肝細胞（N）と類似する．

（図7-B, C）．免疫染色では，ステロイド合成酵素の転写因子であるadrenal 4 binding proteinなどに対する抗体で細胞核が特異的に陽性に染まり，診断的価値が高い．多くは良性の腺腫（副腎腺腫）であるが，悪性と考えられる例も報告されている[18]．組織学的鑑別疾患としては，HCA，脂肪成分を含む高分化型肝細胞癌，血管筋脂肪腫，腎細胞癌などの転移性肝腫瘍が挙げられる．

まとめ

- 肝結節性病変は臨床像および血行動態などを加味し臨床病理学的に診断する必要がある．
- HCAは近年，分子病理学的に亜分類・診断され，免疫染色が病理学的鑑別に有用であるが，従来の診断基準との矛盾症例や非定型例が存在する．
- FNH，FNH-like noduleの肝細胞性過形成結節は，HCAや肝細胞癌などの腫瘍性結節との鑑別が重要である．
- monotypic epithelioid angiomyolipomaなど脂肪成分を欠く，またはとぼしい血管筋脂肪腫は肝細胞癌との組織学的鑑別が困難であるが，HMB45などのメラノーママーカーの免疫染色が診断の決め手となる．
- 腫瘍の一部しかみることができない腫瘍針生検では，診断困難な症例も多い．
- 胆管細胞腺腫は転移性腺癌との鑑別が重要であるが，病理診断は比較的容易である．

■文献

1) Bioulac-Sage P, Balabaud C, Wanless IR: Focal nodular hyperplasia and hepatocellular adenoma. *In* Bosman FT, Carneiro F, Hruban RH, et al (eds): WHO classification of tumors of the digestive system. 4th ed, Lyon, IARC, p.198-204, 2010.
2) Evason KJ, Grenert JP, Ferrell LD, et al: Atypical hepatocellular adenoma-like neoplasms with β-catenin activation show cytogenetic alterations similar to well-differentiated hepatocellular carcinomas. Hum Pathol **44:** 750-758, 2013.
3) Paradis V, Benzekri A, Dargère D, et al: Telangiectatic focal nodular hyperplasia: a variant of hepatocellular adenoma. Gastroenterology **126:** 1323-1329, 2004.
4) Bioulac-Sage P, Rebouissou S, Sa Cunha A, et al: Clinical, morphologic, and molecular features defining so-called telangiectatic focal nodular hyperplasias of the liver. Gastroenterology **128:** 1211-1218, 2005.
5) Maylee H, Harada K, Igarashi S, et al: Case of telangiectatic/inflammatory hepatocellular adenoma arising in a patient with primary sclerosing cholangitis. Hepatol Res **42:** 611-618, 2012.
6) 奥平定之: Focal nodular hyperplasia 23切除例の臨床病理学的検討. 肝臓 **34:** 621-629, 1993.
7) Cherqui D, Rahmouni A, Charlotte F, et al: Management of focal nodular hyperplasia and hepatocellular adenoma in young women: a series of 41 patients with clinical, radiological, and pathological correlations. Hepatology **22:** 1674-1681, 1995.
8) Vilgrain V, Fléjou JF, Arrivé L, et al: Focal nodular hyperplasia of the liver: MR imaging and pathologic correlation in 37 patients. Radiology **184:** 699-703, 1992.
9) Wanless IR, Mawdsley C, Adams R: On the pathogenesis of focal nodular hyperplasia of the liver. Hepatology **5:** 1194-1200, 1985.
10) Nguyen BN, Fléjou JF, Terris B, et al: Focal nodular hyperplasia of the liver: a comprehensive pathologic study of 305 lesions and recognition of new histologic forms. Am J Surg Pathol **23:** 1441-1454, 1999.
11) Lepreux S, Laurent C, Balabaud C, et al: FNH-like nodules: possible precursor lesions in patients with focal nodular hyperplasia (FNH). Comp Hepatol **2:** 7, 2003.
12) Terada T, Kitani S, Ueda K, et al: Adenomatous hyperplasia of the liver resembling focal nodular hyperplasia in patients with chronic liver disease. Virchows Arch A Pathol Anat Histopathol **422:** 247-252, 1993.
13) Kim SR, Maekawa Y, Ninomiya T, et al: Multiple hypervascular liver nodules in a heavy drinker of alcohol. J Gastroenterol Hepatol **20:** 795-799, 2005.
14) Yamasaki S, Tanaka S, Fujii H, et al: Monotypic epithelioid angiomyolipoma of the liver. Histopathology **36:** 451-456, 2000.
15) Bhathal PS, Hughes NR, Goodman ZD: The so-called bile duct adenoma is a peribiliary gland hamartoma. Am J Surg Pathol **20:** 858-864, 1996.
16) Liu Q, Liu J, Chen W, et al: Primary solitary fibrous tumors of liver: a case report and literature review. Diagn Pathol **8:** 195, 2013.
17) 矢野博久, 中島　収, 島松一秀: 血管・間葉系腫瘍およびその他. 中沼安二, 坂元亨宇 (編): 腫瘍病理鑑別診断アトラス肝癌. 文光堂, p.164-173, 2010.
18) Schechter DC: Aberrant adrenal tissue. Ann Surg **167:** 421-426, 1968.

Summary

Pathology of Benign Tumors of the Liver

Kenichi Harada*

Hepatic nodular lesions include various types of neoplastic, hyperplastic, and hamartomatous lesions as well as hepatocellular carcinoma and cholangiocarcinoma. Most lesions are pathologically easy to diagnose, but some require clinicopathological diagnosis with consideration of clinical and radiological features. Moreover, it has recently become possible to classify and diagnose hepatocellular adenoma based on the pattern of gene mutation and associated immunohistochemical features. In future, pathologists must match the classical pathological diagnosis with the genetic criteria for hepatocellular adenoma.

*Department of Human Pathology, Kanazawa University Graduate School of Medical Sciences

OPEN ACCESS Freely available online

PLOS ONE

Activation of the PI3K/mTOR Pathway Is Involved in Cystic Proliferation of Cholangiocytes of the PCK Rat

Xiang Shan Ren[1,2], Yasunori Sato[1], Kenichi Harada[1], Motoko Sasaki[1], Shinichi Furubo[1], Jing Yu Song[2], Yasuni Nakanuma[1,3]*

1 Department of Human Pathology, Kanazawa University Graduate School of Medicine, Kanazawa, Japan, **2** Department of Pathology, Yanbian University College of Medicine, Yanji-city, China, **3** Department of Pathology, Shizuoka Cancer Center, Shizuoka, Japan

Abstract

The polycystic kidney (PCK) rat is an animal model of Caroli's disease as well as autosomal recessive polycystic kidney disease (ARPKD). The signaling pathways involving the mammalian target of rapamycin (mTOR) are aberrantly activated in ARPKD. This study investigated the effects of inhibitors for the cell signaling pathways including mTOR on cholangiocyte proliferation of the PCK rat. Cultured PCK cholangiocytes were treated with rapamycin and everolimus [inhibitors of mTOR complex 1 (mTOC1)], LY294002 [an inhibitor of phosphatidylinositol 3-kinase (PI3K)] and NVP-BEZ235 (an inhibitor of PI3K and mTORC1/2), and the cell proliferative activity was determined in relation to autophagy and apoptosis. The expression of phosphorylated (p)-mTOR, p-Akt, and PI3K was increased in PCK cholangiocytes compared to normal cholangiocytes. All inhibitors significantly inhibited the cell proliferative activity of PCK cholangiocytes, where NVP-BEZ235 had the most prominent effect. NVP-BEZ235, but not rapamycin and everolimus, further inhibited biliary cyst formation in the three-dimensional cell culture system. Rapamycin and everolimus induced apoptosis in PCK cholangiocytes, whereas NVP-BEZ235 inhibited cholangiocyte apoptosis. Notably, the autophagic response was significantly induced following the treatment with NVP-BEZ235, but not rapamycin and everolimus. Inhibition of autophagy using siRNA against protein-light chain3 and 3-methyladenine significantly increased the cell proliferative activity of PCK cholangiocytes treated with NVP-BEZ235. In vivo, treatment of the PCK rat with NVP-BEZ235 attenuated cystic dilatation of the intrahepatic bile ducts, whereas renal cyst development was unaffected. These results suggest that the aberrant activation of the PI3K/mTOR pathway is involved in cystic proliferation of cholangiocytes of the PCK rat, and inhibition of the pathway can reduce cholangiocyte proliferation via the mechanism involving apoptosis and/or autophagy.

Citation: Ren XS, Sato Y, Harada K, Sasaki M, Furubo S, et al. (2014) Activation of the PI3K/mTOR Pathway Is Involved in Cystic Proliferation of Cholangiocytes of the PCK Rat. PLoS ONE 9(1): e87660. doi:10.1371/journal.pone.0087660

Editor: Jin Q. Cheng, H. Lee Moffitt Cancer Center & Research Institute, United States of America

Received July 25, 2013; **Accepted** December 28, 2013; **Published** January 30, 2014

Copyright: © 2014 Ren et al. This is an open-access article distributed under the terms of the Creative Commons Attribution License, which permits unrestricted use, distribution, and reproduction in any medium, provided the original author and source are credited.

Funding: This study was supported by Grants-in-Aid from the Ministry of Health, Labor, and Welfare, Japan (Y. S.). The funders had no role in study design, data collection and analysis, decision to publish, or preparation of the manuscript.

Competing Interests: The authors have declared that no competing interests exist.

* E-mail: nakanuma@staff.kanazawa-u.ac.jp

Introduction

Caroli's disease is characterized by the progressive, multiple cystic dilatation of intrahepatic bile ducts, and is frequently associated with portal fibrosis corresponding to congenital hepatic fibrosis [1]. It belongs to a group of congenital hepatorenal fibrocystic syndrome, and is a hepatic manifestation of autosomal recessive polycystic kidney disease (ARPKD) [2]. The polycystic kidney (PCK) rat is an established animal model of Caroli's disease with congenital hepatic fibrosis as well as ARPKD [3]. Using the PCK rat, potential therapeutic strategies for Caroli's disease and ARPKD have been analyzed. However, no effective therapy applicable to human disease has been established [4].

The mammalian target of rapamycin (mTOR) has attracted attention because of its involvement in a variety of diseases including cancer [5]. The mTOR functions as two distinct multiprotein complexes, mTOR complex 1 (mTORC1) and complex 2 (mTORC1). The mTORC1 phosphorylates S6 kinase (S6) and eukaryotic initiation factor 4E-binding protein-1 (4E-BP1), and regulates cell growth, proliferation, and survival. The mTORC2 has been suggested that it lies downstream of phosphatidylinositol 3-kinase (PI3K) signaling and phosphorylates Akt on Ser473, although it is less well studied in contrast to mTORC1.

Rapamycin and its analog, everolimus, are inhibitors of mTORC1, and have antitumor effects in various cancers by inhibiting cell proliferation, and by affecting apoptosis and autophagy. The rapamycin-sensitive mTORC1 contains phosphorylated (p)-Ser2448, which is consistent with Ser2448 phosphorylation being sensitive to acute rapamycin treatment. The rapamycin-insensitive mTORC2 complex contains p-Ser2481, which is consistent with Ser2481 being a rapamycin-insensitive autophosphorylation site [6].

Rapamycin have been shown to be effective in rodent models of autosomal dominant PKD (ADPKD), which is consistent with the findings showing that the PI3K/Akt/mTOR pathway is aberrantly activated in ADPKD [7–11]. However, in clinical trials, rapamycin and everolimus have not shown benefit in patients with ADPKD [12,13]. Similarly, rapamycin failed to attenuate progression of kidney and liver lesions in the PCK rat in vivo, although the activation of Akt/mTOR pathway has been observed in patients with ARPKD [14,15]. Thus, the clinical application of mTORC1 inhibitors to PKD patients seems to be limited of use.

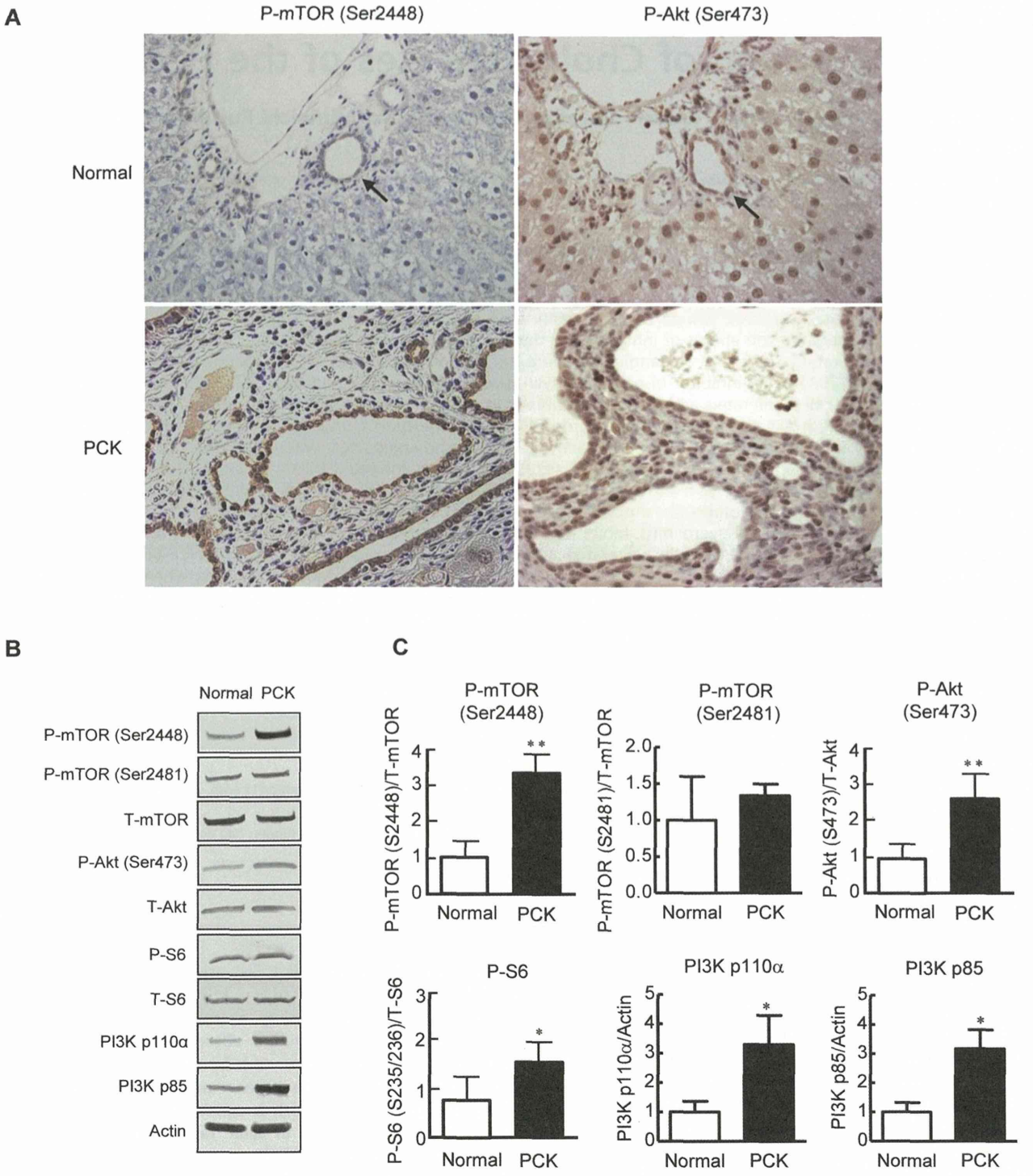

Figure 1. Overexpression of p-mTOR, p-Akt, p-S6, and PI3K in PCK cholangiocytes. The immunohistochemical expression of p-mTOR (Ser2448) and p-Akt (Ser473) was examined using liver sections of 10-month-old rats. Increased expression of p-mTOR (Ser2448) and p-Akt (Ser473) was observed in bile duct epithelium of the PCK liver compared to that of the normal liver (A). Western blot analysis using protein extracts from cultured cholangiocytes showed that the expression p-mTOR (Ser2448), p-mTOR (Ser2481), p-Akt (Ser473), p-S6, PI3K p110α, and PI3K p85 was increased in PCK cholangiocytes compared to normal cholangiocytes (B). The results of the semiquantitative analysis of Western blotting are shown in C. Arrows indicate interlobular bile ducts of the normal liver. *, $p<0.01$; **, $p<0.05$ (vs. normal cholangiocytes). Original magnifications; x400 (A).
doi:10.1371/journal.pone.0087660.g001

Recently, multi-targeting approach against the PI3K/mTOR pathway has provided novel tools for elucidation of the roles of mTOR and mTOR-based therapeutic strategy. NVP-BEZ235 belongs to the class of imidazoquinolines, and is a novel inhibitor of PI3K and mTORC1/2 [5]. In a certain type of human neoplastic cells, NVP-BEZ235 suppresses cell proliferation by inducing apoptosis or autophagy [16,17], but its therapeutic benefits for the pathogenesis of PKD have not been tested.

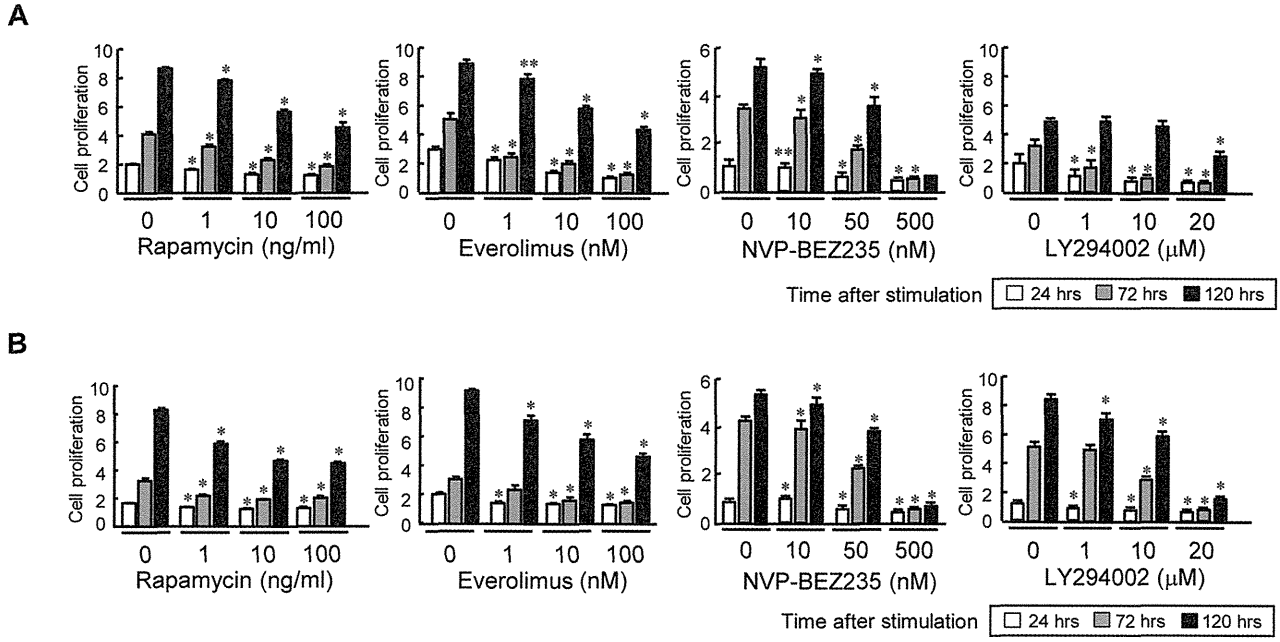
A
Cell proliferation
0 1 10 100
Rapamycin (ng/ml)
0 1 10 100
Everolimus (nM)
0 10 50 500
NVP-BEZ235 (nM)
0 1 10 20
LY294002 (μM)
Time after stimulation
24 hrs
72 hrs
120 hrs
B
Cell proliferation
0 1 10 100
Rapamycin (ng/ml)
0 1 10 100
Everolimus (nM)
0 10 50 500
NVP-BEZ235 (nM)
0 1 10 20
LY294002 (μM)
Time after stimulation
24 hrs
72 hrs
120 hrs

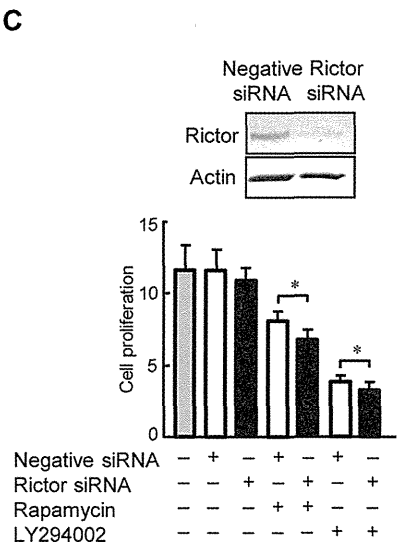
C
Negative Rictor
siRNA siRNA
Rictor
Actin
Cell proliferation
Negative siRNA
Rictor siRNA
Rapamycin
LY294002

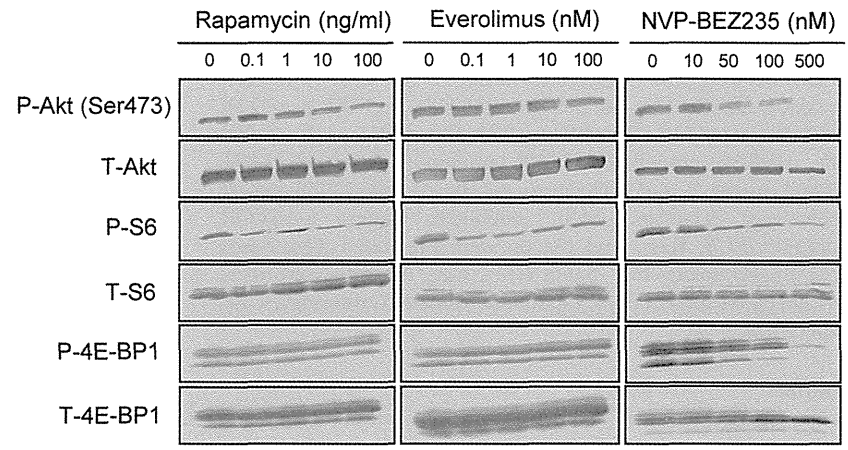
D
Rapamycin (ng/ml)
0 0.1 1 10 100
Everolimus (nM)
0 0.1 1 10 100
NVP-BEZ235 (nM)
0 10 50 100 500
P-Akt (Ser473)
T-Akt
P-S6
T-S6
P-4E-BP1
T-4E-BP1

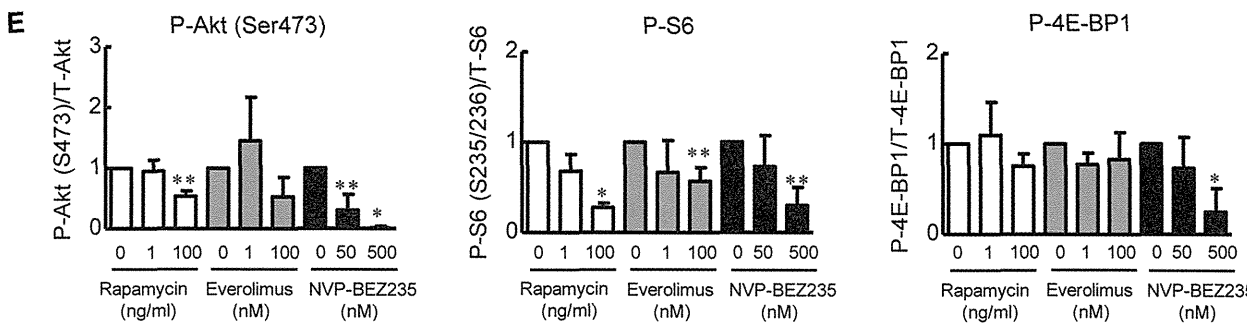
E
P-Akt (Ser473)
P-Akt (S473)/T-Akt
P-S6
P-S6 (S235/236)/T-S6
P-4E-BP1
P-4E-BP1/T-4E-BP1
0 1 100 0 1 100 0 50 500
Rapamycin (ng/ml)
Everolimus (nM)
NVP-BEZ235 (nM)

Figure 2. In vitro effects of PI3K and mTOR inhibitors on cholangiocytes. Normal and PCK cholangiocytes were treated with the PI3K and/or mTOR inhibitors, and the cell proliferative activity was determined using the WST-1 assay as described in the Materials and Methods. Rapamycin, everolimus, NVP-BEZ235 and LY294002 significantly inhibited the cell proliferative activity of normal (A) and PCK (B) cholangiocytes in a dose-dependent fashion, where the most prominent inhibitory effect was observed in both cholangiocytes treated with NVP-BEZ235 for 120 hours. Rictor siRNA significantly reduced the cell proliferative activity of the PCK cholangiocytes when it was used in combination with rapamycin and LY 294002 (C). Western blot analysis showed that the expression of p-Akt (Se473) and p-S6 was reduced following 24 hour-treatment with rapamycin, everolimus and NVP-BEZ235 in a dose-dependent fashion in PCK cholangiocytes (D). The results of the semiquantitative analysis of Western blotting are shown in E. Note that the expression of p-Akt (Ser473) and p-4E-BP1 was markedly decreased in PCK cholangiocytes following the treatment with 500 nM NVP-BEZ235 (D and E). *, $p<0.01$; **, $p<0.05$ (vs. untreated control).
doi:10.1371/journal.pone.0087660.g002

Disturbance in the balance between apoptosis and cell proliferation is a pathologic feature of PKD. Increased apoptosis has been observed in human ADPKD as well as the rodent models of PKD [3,18–21]. Activation of caspase signaling and dysregulation of antiapoptotic bcl-2 protein have been described in PKD. Recently, the role of autophagy has been investigated in mouse models of PKD [22]. However, the pathologic significance of autophagy in the PCK rat is largely unknown.

In this study, the effects of the PI3K and/or mTORC1/2 inhibitors were investigated using the PCK rat to clarify the mechanism of cystic dilatation of the intrahepatic bile ducts and their therapeutic usefulness for the inhibition of bile duct dilatation, particularly focusing on the cell proliferative activity in relation to apoptotic and autophagic responses.

Materials and Methods

Reagents and Antibodies

Rapamycin and everolimus were purchased from Sigma-Aldrich (St. Louis, MO), and 3-methyladenine (3MA) and LY294002 were from Calbiochem (San Diego, CA). Antibodies for Akt, p-Akt (Ser473), S6, p-S6 (Ser235/236), mTOR, p-mTOR (Ser2448), p-mTOR (Ser2481), p-ERK1/2, PI3K p110α, PI3K p85, 4E-BP1, p-4E-BP1(T37/46), protein-light chain3 (LC3), cleaved caspase 3, and Rictor were purchased from Cell Signaling Technology (Danvers, MA). Antibodies against p-mTOR (Ser2448), LC3, Ki-67 and β-actin were purchased from Santa Cruz Biotechnology Inc. (Santa Cruz, CA), Nanotools (Munich, Germany), Nichirei (Tokyo, Japan) and Abcam (Cambridge, UK), respectively.

Animals

The PCK rats were maintained at the laboratory animal institute of Kanazawa University Graduate School of Medicine. Normal (Crj:CD) rats were purchased from Charles River Japan (Sagamihara, Japan). The protocol was approved by the committee of Institute for Experimental Animals, Kanazawa University Advanced Science Research Center (Permit Number: AP-122551). Animal studies were performed in accordance with the guidelines for the Care and Use of laboratory Animals at Takara-machi Campus of Kanazawa University.

Liver Specimens

For immunohistochemical analysis, livers were removed from normal and PCK rats. The liver tissues were immersed in 10% formalin neutral buffer solution (pH 7.4), and embedded in paraffin. More than 10 serial sections, 4 μm thick, were cut from each paraffin block, and were subjected to the analysis.

Cell Culture of Cholangiocytes

Cholangiocytes were isolated, purified, and cultured from the intrahepatic large bile ducts of normal and PCK and rats as described previously [23,24]. The cells were set on cell culture dishes covered with a standard medium composed of Dulbecco's modified Eagle's medium/F-12 (Gibco, Grand Island, NY) containing 10% bovine growth serum (HyClone, Logan, UT), 5 μmol/L forskolin (Wako Pure Chemical Industries, Osaka, Japan), 20 ng/ml of epidermal growth factor (Upstate Biotechnology, Lake Placid, NY) and 1% antibiotics-antimycotic (Life Technologies) at 37°C in an atmosphere of 5% CO_2.

Cell Proliferation Assay

Proliferative activity of cholangiocytes was determined using the WST-1 assay according to the manufacturer's instructions (Roche, Mannheim, Germany). The cells were seeded in 96-well tissue culture plates and maintained for 24 hours with the standard medium. Then the cells were treated with rapamycin, everolimus, NVP-BEZ235 and LY294002 at the concentrations and at the intervals indicated. The WST-1 reagent was added and incubated for 1 hour before reading the plate. Each assay was conducted in six sets.

Three-dimensional Cell Culture

Biliary cyst formation were examined using the three-dimensional cell culture system with the use of the growth factor reduced Matrigel (BD Biosciences, San Jose, CA). On day 6 after the beginning of the cell culture, the culture medium was changed to that containing rapamycin (100 ng/ml), everolimus (100 nM) and NVP-BEZ235 (100 nM). Incubation was continued for further 72 hours. The morphological changes were recorded using a digital camera under phase-contrast microscopy. More than 6 fields at x40 magnification were recorded for each experimental group, and the size of well-developed cysts was analyzed within the field. The size of the same cyst was determined at day 0 (before the treatment) and day 3 (72 hours after the treatment) on the digital images, and the growth rate was calculated.

Quantitative Real-time PCR

Reverse transcriptase-PCR was performed using total RNA (1 μg) extracted from the cholangiocytes. Total RNA was extracted using an RNA extraction kit (RNeasy mini; Qiagen, Tokyo, Japan) and was used to synthesize cDNA with reverse transcriptase (ReverTra Ace; Toyobo, Osaka, Japan). Quantitative real-time PCR was performed according to a standard protocol using the SYBR Green PCR Master Mix (Toyobo Co.) and Mx3000P&Mx3005P Real-Time QPCR System (Applied Biosystems, CA). The sequences of the primers (5′–3′) used were: bcl-2; forward, CTGGCATCTTCTCCTTCCAG; reverse, CGGTAGCGACGAGAGAAGTC: glyceraldehyde-3-phosphate dehydrogenase (GAPDH); forward, GAGTCAACG-GATTTGGTCGT; reverse, TTGATTTTGGAGGGATCTC. Cycling conditions were incubated at 62°C for 2 minutes, 95°C for 10 minutes, 40 cycles of 95°C for 15 seconds and 60°C for 1 minute. Fold difference compared with GAPDH was calculated. Each assay was conducted in three sets.

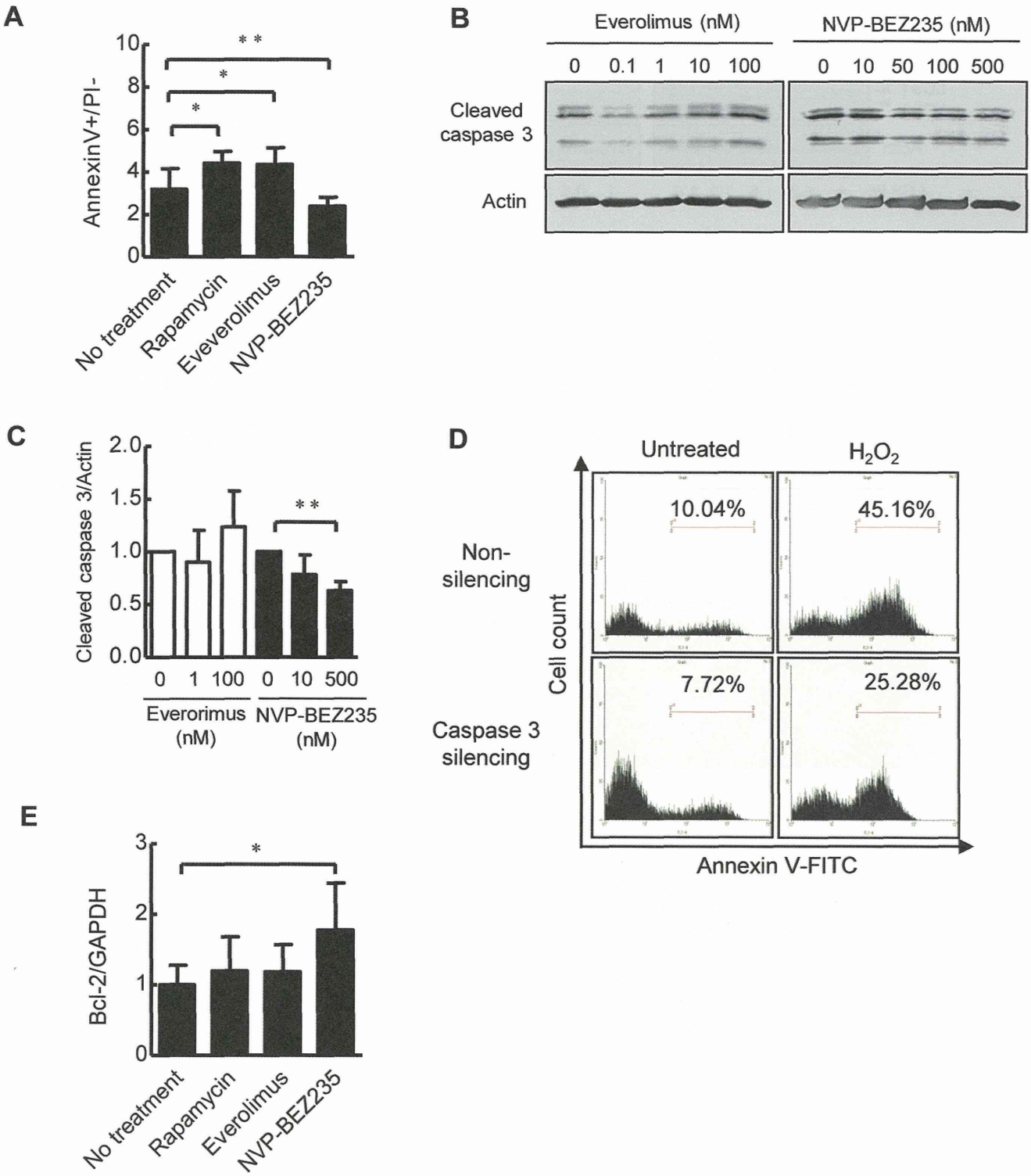

Figure 3. Effects of mTOR inhibitors on cholangiocyte apoptosis in vitro. Apoptosis was determined following the treatment of PCK cholangiocytes with rapamycin (100 ng/ml), everolimus (100 nM) and NVP-BEZ235 (500 nM) as described in the Materials and Methods. Flow cytometric analysis showed that 24-hour treatment with rapamycin and everolimus significantly induced apoptosis in PCK cholangiocytes, while it was significantly inhibited by the treatment with NVP-BEZ235 (A). NVP-BEZ235 significantly reduced the expression of cleaved caspase 3 in PCK cholangiocytes that was determined using Western blot analysis (B). The results of the semiquantitative analysis of Western blotting are shown in C. Flow cytometric analysis showed that silencing of caspase 3 using siRNA in PCK cholangiocytes resulted in the reduction of the percentage of apoptotic cells under normal and H_2O_2-treated conditions (D). The analysis with quantitative real-time PCR showed that treatment with NVP-BEZ235 significantly increased the expression of bcl-2 mRNA in PCK cholangiocytes (E). *, $p<0.01$; **, $p<0.05$ (vs. untreated control).
doi:10.1371/journal.pone.0087660.g003

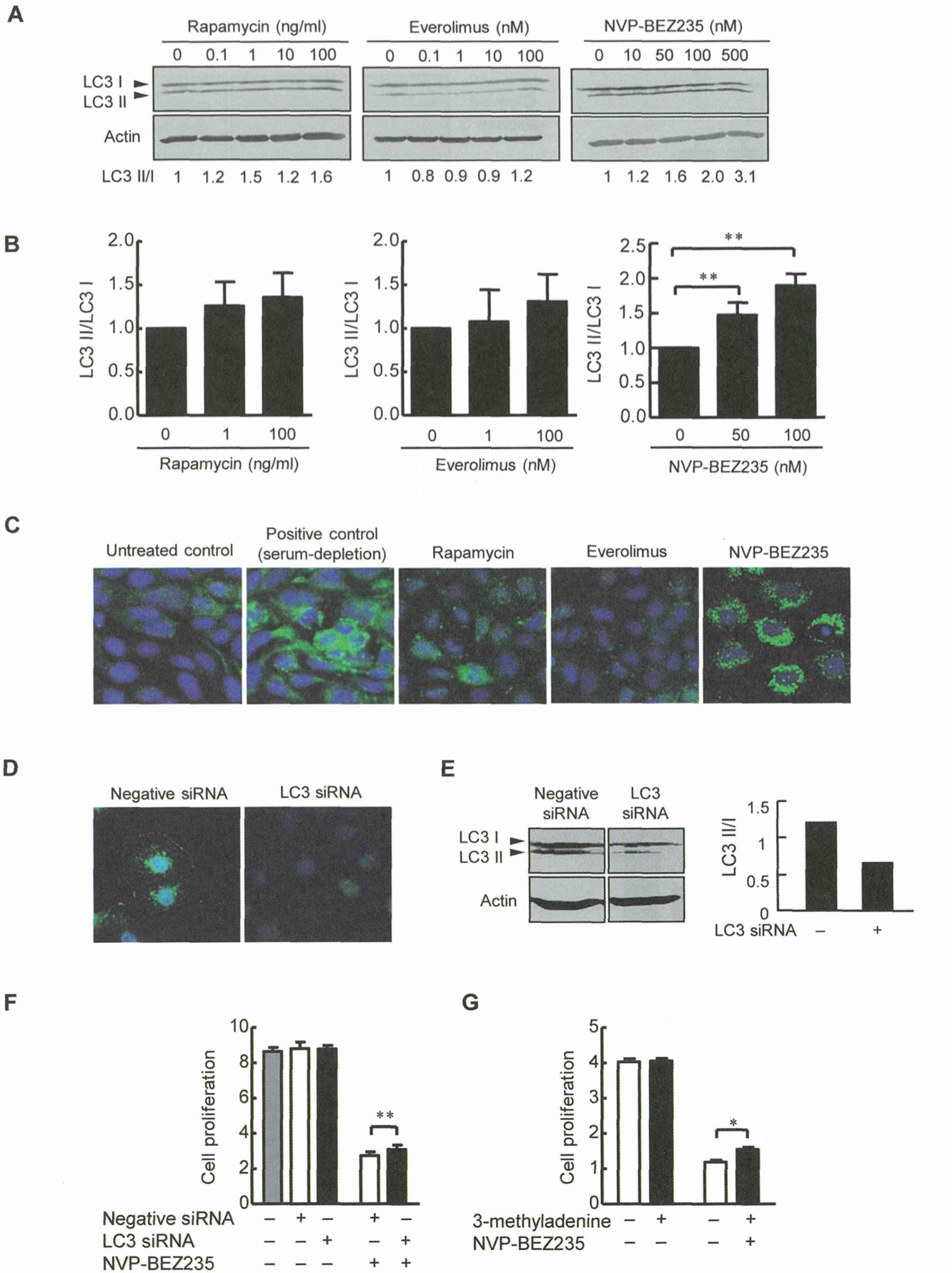
A
Rapamycin (ng/ml)
0 0.1 1 10 100
Everolimus (nM)
0 0.1 1 10 100
NVP-BEZ235 (nM)
0 10 50 100 500
LC3 I
LC3 II
Actin
LC3 II/I 1 1.2 1.5 1.2 1.6
1 0.8 0.9 0.9 1.2
1 1.2 1.6 2.0 3.1
B
LC3 II/LC3 I
Rapamycin (ng/ml)
Everolimus (nM)
NVP-BEZ235 (nM)
C
Untreated control
Positive control (serum-depletion)
Rapamycin
Everolimus
NVP-BEZ235
D
Negative siRNA
LC3 siRNA
E
Negative siRNA
LC3 siRNA
LC3 I
LC3 II
Actin
LC3 II/I
F
Cell proliferation
Negative siRNA
LC3 siRNA
NVP-BEZ235
G
Cell proliferation
3-methyladenine
NVP-BEZ235

Figure 4. Effects of mTOR inhibitors on cholangiocyte autophagy in vitro. PCK cholangiocytes were treated with rapamycin, everolimus and NVP-BEZ235 for 24 hours, and autophagy of the cells was detected by the conversion of LC3 I to LC3 II using Western blot analysis. NVP-BEZ235 induced a dose-dependent increase in the autophagy-specific LC3 II form, while rapamycin and everolimus did not significantly induce autophagy in PCK cholangiocytes (A). The results of the semiquantitative analysis of Western blotting are shown in B. Immunocytochemistry of LC3 showed the induction of autophagy by NVP-BEZ235 in PCK cholangiocytes (C). Silencing of LC3 was performed using LC3 siRNA in PCK cholangiocytes, and immunocytochemistry (D) and Western blot analysis (E) showed that LC3 siRNA reduced LC3 II formation in the cholangiocytes. When PCK cholangiocytes were treated with NVP-BEZ235 (100 nM) for 48 hours, the cell proliferative activity of the LC3 siRNA-treated cells was significantly high than those without LC3 siRNA treatment that was determined using the WST-1 assay (F). Following 48-hour treatment of PCK cholangiocytes with 3-methyladenine (500 nM) together with NVP-BEZ235 (100 nM), the cell proliferative activity was significantly increased compared to those with NVP-BEZ235 alone (G). Original magnifications, x1000 (C and D). *, $p<0.01$; **, $p<0.05$ (vs. untreated control).
doi:10.1371/journal.pone.0087660.g004

Western Blot Analysis

Total proteins were extracted from the cells using T-PER protein extraction reagent (Pierce Chemical Co., Rockford, IL). The protein was subjected to 10% SDS-polyacrylamide electrophoresis, and then electrophoretically transferred on to a nitrocellulose membrane. The membrane was incubated with primary antibodies against Akt (1:1000), p-Akt (Ser473) (1:1000), S6 (1:500), p-S6 (1:500), mTOR (1:500), p-mTOR (Ser2448) (1:500; Cell Signaling Technology), p-mTOR (Ser2481) (1:500), p-ERK1/2 (1:500), PI3K p110α (1:500), PI3K p85 (1:500), 4E-BP1 (1:1000), p-4E-BP1 (T37/46) (1:1000), cleaved caspase 3 (1:400), LC3 (1:500; Cell Signaling Technology), and Rictor (1:500). The protein expression was detected using an EnVision+system (DakoCytomation, Glostrup, Denmark). 3,3′-diaminobenzidine tetrahydrochloride (DAB) was used as the chromogen. Semiquantitative analysis of the results was performed for three independent experiments using NIH J image software (National Institutes of Health, Bethesda, MD).

Apoptosis Assay

Flow cytometric analysis of apoptosis was performed by the quantitative detection of phosphatidylserine of the cell surface using Annexin V/FITC and PI apoptosis detection kit (BD Biosciences, San Jose, CA). Cultured cholangiocytes were treated with rapamycin (100 ng/ml), everolimus (100 nM), and NVP-BEZ235 (500 nM) for 24 hours. The cells were washed twice with cold phosphate-buffered saline, and suspended in binding buffer. The cell suspension (100 µl) was incubated with Annexin V-FITC (5 µl) and propidium iodide (PI) (2 µl) for 15 minutes at room temperature. Then binding buffer (400 µl) was added in the cell suspension, and the samples were analyzed within 1 hour using flow cytometer (JASAN, Bay bioscience, Kobe, Japan). Apoptotic cells were expressed by the percentage of Annexin V-FITC positive-, PI negative-cells of total gated cells. The experiments were performed in three sets for each condition. Apoptosis positive control cells were treated with 200 µM H_2O_2 for 24 hours.

For the detection of apoptotic cells in paraffin-embedded tissue sections, a terminal dUTP nick-end labeling (TUNEL) method was used. After proteinase K digestion and endogenous peroxidase blocking, the sections were stained by using a commercial kit (TdT-FragEL DNA fragmentation detection kit, Calbiochem). After color development with DAB, sections were counterstained with methyl green.

Transfection of siRNA

Synthetic siRNA for LC3, caspase 3 and Rictor, and non-silencing siRNA (negative control) were purchased from Qiagen (Tokyo, Japan). Transfections of siRNA were performed using HiPerFect Transfection Reagent (Qiagen) according to the manufacturer's instructions. Cholangiocytes were incubated for 24 hour with the standard medium. After removal of the medium, the cells were incubated with Dulbecco's modified Eagle's medium/F-12 (Gibco) containing premixed siRNA (10 nM) and 3 µl of HiPerFect Transfection Reagent, and were further incubated for 72 hours.

Immunofluorescence Confocal Microscopy

Cholangiocytes were seeded in slide chamber, and were treated with rapamycin (100 ng/ml), everolimus (100 nM), and NVP-BEZ235 (500 nM) for 24 hours. They were fixed with 4% paraformaldehyde for 15 minutes, and were permeabilized for 10 minutes with 0.1% Triton X-100. After blocking, the cells were incubated with a primary antibody against LC3 (1:200; Cell Signaling Technology) for overnight at 4°C. Alexa-488 (10 µg/ml; Molecular Probes, Eugene, OR) was used as a secondary antibody, and nuclei were stained with 4′6-diamidino-2-phenylindole. Positive control of autophagy was the cells incubated with serum-free medium for 24 hours.

Immunohistochemistry

After deparaffinization of the sections, antigen retrieval was performed by microwaving in 10 mmol/L citrate buffer (pH 6.0) for p-Akt, p-S6 and LC3 staining, and by heating in Tris-ethylenediaminetetraacetic acid buffer (pH 9.0) with a pressure cooker for p-mTOR and Ki-67 staining. After blocking the endogenous peroxidase, the sections were incubated overnight at 4°C with anti-p-mTOR (Ser2448) (1:20; Santa Cruz Biotechnology, Inc.), anti-p-Akt (Ser473) (1:25), anti-p-S6 (1:200), anti-LC3 (1:100; Nanotools) and anti-Ki-67 (pre-diluted) antibodies. Then the sections were incubated with the secondary antibody conjugated to the peroxidase-labeled polymer, EnVison+system (DakoCytomation). Color development was performed using DAB, and the sections were counterstained with hematoxylin. Control sections were evaluated by substitution of the primary antibodies with nonimmunized serum without signal detection.

In vivo Administration of NVP-BEZ235

A total of 22 male rats were used. At 4 weeks of age, 11 normal and 11 PCK rats were divided into control and experimental groups. The experimental groups were intraperitoneally administrated 20 mg/kg NVP-BEZ235 daily between 4 and 8 weeks of age. The dosage was determined based on the previous report [25]. The control group received vehicle (2% Tween 80 and 1% methylcellulose in water) alone. At 8 weeks of age, rats were weighed and anesthetized with diethyl ether. Blood was obtained by puncture of inferior vena cava for hematological analysis. The liver and kidney were weighed and immersed in 10% formalin neutral buffer solution (pH 7.4), and the tissues were embedded in paraffin for histological analysis.

Histological Assessment

Paraffin-embedded sections were prepared for the liver and kidney, and whole tissue sections were used to measure cyst volumes and liver fibrosis. Cyst volumes of the liver and kidney were assessed using hematoxylin-eosin stained sections. Liver